AIMS Mathematics, 8(1): 792–814.
DOI: 10.3934/math.2023039
Received: 17 August 2022
Revised: 12 September 2022
Accepted: 18 September 2022
Published: 12 October 2022

http://www.aimspress.com/journal/Math

*Research article*

# Solitary wave solutions in time-fractional Korteweg-de Vries equations with power law kernel

**Khalid Khan**[1], **Amir Ali**[1,*], **Muhammad Irfan**[2] **and Zareen A. Khan**[3]

[1] Department of Mathematics, University of Malakand, Khyber Pakhtunkhwa, Pakistan

[2] Department of Physics, University of Malakand, Khyber Pakhtunkhwa, Pakistan

[3] Department of Mathematical Sciences, College of Science, Princess Nourah bint Abdulrahman University, P.O. Box 84428, Riyadh 11671, Saudi Arabia

* **Correspondence:** Email: amiralishahs@yahoo.com.

**Abstract:** The non-linear time-fractional Korteweg-de Vries and modified Korteweg-de Vries equations are studied with Caputo's fractional derivative. The general higher-order solitary wave solutions are derived using a novel technique called the Aboodh transform decomposition method. To validate the obtained results, two examples of Caputo's fractional derivative with appropriate subsidiary conditions are illustrated. The accuracy and efficiency are confirmed by using numerical simulations and error analysis, where good agreements are obtained. The numerical analysis shows that, in comparison to the time-fractional Korteweg-de Vries solution, the solitary wave solution for the time-fractional modified Korteweg-de Vries equation is less stable against the oscillations. The variations in the temporal variable $t$ enhance the strength of the wave solutions. Moreover, the wave perturbations taper off as $t$ attains large values. The parameter $\alpha$ signifies the fractional derivative influence on the wave dispersion and nonlinearity effects. This affects the amplitude as well as the spatial extension of the solitary waves. With a relatively small value of $t$, the obtained solutions admit pulse-shaped solitons. Moreover, the wave's solutions suffer from oscillations when the temporal variable attains large values. This effect cannot be noticed in the soliton solutions obtained in the integer order systems.

**Keywords:** non-linear time-fractional KdV; Caputo's fractional derivative; Aboodh transform; decomposition method; soliton solutions
**Mathematics Subject Classification:** 35Bxx, 35Qxx, 35Axx, 37Mxx, 65R10, 06A33, 42A38, 74-XX

## 1. Introduction

Currently, fractional-order calculus (FOC) plays a dynamic role in the development and applications of modern science and technology [1]. The FOC is a field of mathematics that deals with differentiation and integration under an arbitrary order of the operation; the order is not limited to the integer one but can also be any real or even complex number [2–4]. For a long time, it was ignored due to the integral complexity and freedom of integer order calculus, as well as the reality that FOC does not have entirely conventional physical or geometrical understandings [5]. Currently, there is a strong interest in generalising integer-order NPDEs to model complex engineering problems such as bio-engineering, electronics, viscoelasticity, control theory, thermal sciences, electrical networking, chemical, and fluid dynamics [6, 7].

Korteweg-de Vries (KdV) equation has been extensively investigated in physics to describe the interaction and evaluation of non-linear waves. It was originally derived by D. J. Korteweg and G. de Vries, in an investigation to re-generate the solitary waves that govern a small amplitude in one dimension with lengthy propagating gravity waves spreading in a shallow channel of water [8]. Apart from solitary waves, the KdV equation has also been studied for numerous physical phenomena, including hydro-magnetic waves, lattice dynamics, physics of plasma such as electron-acoustic (EA) and ion-acoustic (IA) waves [9]. It is also used in aerodynamics, fluid dynamics, transportation of mass, boundary layer behavior, and modeling the mechanical behavior of materials modeled as a continuous mass for shock wave formations. The concept of excitation of the electron-acoustic (EA) mode was initially proposed by Fried and Gould in the reference [10]. They have noted that the Landau's dampening effect on the EA potentials weakens with increasing wave number. In further experiments, weak dampening of the EA in plasma containing both high- and low-temperature electrons was found to be caused by [11]. Such plasma circumstances had previously been noted in a number of contexts, including [12]. Iwamoto [13] has studied the development of the high frequency Langmuir mode and the electron-acoustic wave evolution in nonrelativistic electron-positron plasma. It has been demonstrated that, in compared to the Langmuir wave, the low frequency EA excitation Landau damped with a substantially higher growth rate. The propagation of electron acoustic waves (EAWs) in plasmas and in space environments has drawn a lot of interest due to its value in comprehending a variety of collective processes in laboratory equipment [14, 15]. Irfan et al. [16] studied fast (Langmuir) and slow (electron-acoustic) modes in dense electron-positron-ions (EPI) plasma. They observed that there is a chance that the fast electron-acoustic (FEA) mode could occur. The slow electron-acoustic (SEA) solitons are not allowed to propagate because they have a negative phase dispersion impact. The EPI plasma may allow for the evolution of electron-holes at a relatively low positron concentration, leading to the formation of compressive FEA solitons. Broadband electrostatic noise (BEN) emissions in the auroral and other regions of the magnetosphere, such as the plasma sheet boundary layer (PSBL) and the polar cusp, have been detected by satellite data. The Korteweg-de Vries (KdV) equation is obtained from studies of small-amplitude EAWs in unmagnetized plasma using first-order reductive perturbation theory [17]. More than 20 percent of the solitary waves' amplitude is understated by the first order soliton solution. Consequently, higher-order fixes may be used to help solve this issue. Shewy et al. [18, 19] investigated the contributions of higher-order corrections to the properties of electrostatic EAWs as well as the impacts of non-thermal distribution of hot electrons. The higher-order correction contribution is given by the time-fractional

modified Korteweg-de Vries (TF-mKdV) which modulates the amplitude of the solitary wave.

The time-fractional modified KdV (TF-mKdV) equation is well-known for its contribution in the creation of the Lax pair and an unlimited quantity of conservation laws for the KdV equation [20]. The finite-gap integration approach and Whitham modulation theory are used to investigate the comprehensive classification of solutions to the defocusing complex modified KdV equation with step-like initial condition [21]. Wang et al. [22] employed the nonlinear steepest descent method of Deift and Zhou, the long-time asymptotics of the focusing Kundu-Eckhaus equation with nonzero boundary conditions at infinity. The TF-mKdV equation is obtained using perturbation expansions and the theory that the soliton width is modest in comparison to the plasma inhomogeneity scale length. In this case, the soliton retains its whole identity, as well as its amplitude, breadth, and speed. Further, Breathers and the unique soliton behavior of the TF-mKdV equation are well-known. Here, we study the localized solutions for time-fractional Korteweg-de Vries (TF-KdV) and time-fractional modified Korteweg-de Vries (TF-mKdV) with help of an analytical method called Aboodh transform decomposition method (ADM) given in [23].

From the conventional Fourier integral, the Aboodh transform is derived. The Aboodh transform was first proposed by Khalid Aboodh [24] to show how to solve various ordinary differential equations in the time domain. This was done because of the Aboodh transform's mathematical features and simplicity. Differential equations are typically solved using Fourier, Laplace, Elzaki, and Sumudu transforms as the primary mathematical methods. Motivated from these study we are interesting to apply the Aboodh transform together with decomposition method to find an approximate solution of our proposed model. The proposed models have been extensively used in modeling complex physical systems such as thermal as well as current flows in electric circuits. It also plays an important role in modeling particles vibrating in their lattices. It should be noted that the physical phenomena in the KdV equation will be considered as non-conservative to describe fractional differential equations. Recently, the time-fractional KdVB equation together with nonlinearities has been extensively investigated using various methods [25]. We consider the integer order of the time derivative term of the mKdV model given in [26] be in the arbitrary order of the following form

$$\frac{\partial^{\alpha} u}{\partial t^{\alpha}} + a\, u^{m} \frac{\partial u}{\partial x} + b\, \frac{\partial^{3} u}{\partial x^{3}} = 0, \quad 0 < \alpha \leq 1, \tag{1.1}$$

with

$$u(x, 0) = f(x), \tag{1.2}$$

the numbers $a, b \in \mathbb{R}$ with $a$ is the non-linearity coefficient and $b$ is the dispersive coefficient of Eq (1.1) and the time fractional-order ($0 < \alpha \leq 1$) derivative is supposed to be in Caputo's form. Equation (1.1) is known as time-fractional modified Korteweg-de Vries (TF-mKdV) equation and is used vastly in plasma physics to study solitary and shock waves [27]. When $m = 1$, the TF-mKdV reduce to simple time fractional Korteweg-de Vries (TF-KdV) equation.

Recently, various descriptions for fractional-order operators are also broadly studied, for example, Caputo-Fabrizio (C-F), Liouville-Caputo, and Riemann-Liouville (R-L) [28]. The R-L derivatives involve the complexity of the assumed function with the power-law kernel, while, the LC derivatives include the complexity of the confined derivative of a considered problem with power-law. Recently, the fractional KdV type equations together with several other nonlinear systems involving the

time-fractional order derivatives along various methods for their analytical solutions have been investigated. To investigate analytical as well as numerical solutions to FNPDEs/TF-mKdV equations, various techniques have been studied [29–31]. Here, we apply the Aboodh decomposition method (ADM) [23] to find an approximate solution of Eq (1.1) in Caputo's sense. The rest of the article is prepared as follows. The preliminaries section 2 includes the main definitions, remarks, and some important results regarding the proposed method. In section 3, the Aboodh transform and Aboodh decomposition method are discussed. In section 4, uniqueness and convergence analysis of the method is discussed. In section 5, we consider two examples in Caputo's form of TF-KdV and TF-mKdV equations with the application of the proposed method. This section also includes numerical solutions and discussion. In section 5, the accuracy and effectiveness of the ADM are confirmed by using the error analysis. We include the summary in section 6, while in section 7 we have given the future work and extension of our present work.

## 2. Preliminaries

In this section, we provide some basic definitions, theorems, lemmas, and remarks, which are essential for our proposed method. We also define some basic rules and definitions related to the Aboodh transform and decomposition methods with some related properties. The Aboodh transform (see the reference [32]) is defined for the functions of exponential order in the following set

$$\mathcal{A} = \{u(t) : \exists\ M, k_1, k_2,\ |u(t)| \leq M\, e^{-vt},\ \ k_1 \leq v \leq k_2\}, \tag{2.1}$$

the constant $M$ must be a finite value for a given function $u(t)$ in the set $\mathcal{A}$, while $k_1, k_2 \in \mathbb{R}$. The Aboodh transform $\mathcal{A}\, u(t)$ is given by

$$\mathcal{A}(u(t))(v) = K(v) = \frac{1}{v}\int_0^\infty u(t)e^{-vt}dt, \qquad t \geq 0, \tag{2.2}$$

where $v \in [k_1, k_2]$ is the variable utilised to factor the variable $t$ in the function $u(.)$.

**Definition 1.** [33] The Aboodh transform for two variables function $x \geq 0$, $t \geq 0$ is defined by

$$\mathcal{A}(u(x,t))(u,v) = K(u,v) = \frac{1}{uv}\int_0^\infty \int_0^\infty e^{-ut}\, e^{-vt} u(x,t)dxdt, \tag{2.3}$$

while the inverse Aboodh transform is give by

$$u(x,t) = \mathcal{A}^{-1}\{K(u,v)\} = \frac{1}{2\pi\, i}\int_{\beta-i\infty}^{\beta+i\infty} u\, e^{ut}\Big[\frac{1}{2\pi\, i}\int_{\gamma-i\infty}^{\gamma+i\infty} ve^{vx}K(u,v)\, dv\Big]du,$$

where, $K(u,v)$, is a function such that $u$ and $v$ defined such that $Re\ (u) \geq \beta$ and $Re\ (v) \geq \gamma$. It should be noted that $\beta, \gamma \in \mathbb{R}$ to be considered accordingly.

**Definition 2.** [34] The Caputo's derivative for $\alpha > 0$ for $u(t)$ is defined by function $u : (0, \infty) \to \mathbb{R}$ is given by

$$^{c}D^{\alpha}u(t) = \frac{1}{\Gamma(n-\alpha)} \int_0^t (t-s)^{n-\alpha-1} u^n(s) ds, \tag{2.4}$$

where $\alpha \in (n-1, n]$, with $n = [\alpha] + 1$, $[\alpha]$ represent the integer part of a real number $\alpha$, providing that the right-hand side of the above integral is continuously well-defined on $(0, \infty)$.

**Definition 3.** [35] Applying Aboodh transform on function $u(x, t)$ in the Caputo's sense is given by

$$\mathcal{A}\{^{c}D^{\alpha}u(x,t)\} = v^{\alpha}K(u,v) - \sum_{k=0}^{n-1} \frac{u^{(k)}(x,0)}{v^{2-\alpha+k}}. \tag{2.5}$$

**Definition 4.** [35] The Aboodh transform of some other functions and derivatives are given as

$$\mathcal{A}\{t^n\} = \frac{n!}{v^{n+2}}, \quad n \in N, \quad \mathcal{A}\{t^{\alpha}\} = \frac{\Gamma(\alpha+1)}{v^{\alpha+2}}, \quad \alpha \geq -1.$$

## 3. Aboodh transform decomposition method

Here, we introduce ADM applied to attain a series of solutions of NODEs and NPDEs. It is a very much effective technique to find an approximate solution of dynamical systems. Writing Eq (1.1) in Caputo's sense, we obtain

$$^{c}D_t^{\alpha}\, u + a\, u^m \frac{\partial u}{\partial x} + b\, \frac{\partial^3 u}{\partial x^3} = 0, \tag{3.1}$$

$0 < \alpha \leq 1$ and

$$u(x, 0) = f(x). \tag{3.2}$$

Using ADM and the definitions given in the previous section, we obtain

$$\mathcal{A}\{^{c}D_t^{\alpha}\, u\} + a\mathcal{A}\{u^m \frac{\partial u}{\partial x}\} + b\mathcal{A}\{\frac{\partial^3 u}{\partial x^3}\} = 0. \tag{3.3}$$

Applying the technique given in section 2 for ADM on fractional order, we obtain

$$\mathcal{A}\{u(x,t)\} = \frac{1}{v^2}\mathcal{A}\{u(x,0)\} - a\frac{1}{v^{\alpha}}\mathcal{A}\{u^m \frac{\partial u}{\partial x}\} - b\frac{1}{v^{\alpha}}\mathcal{A}\{\frac{\partial^3 u}{\partial x^3}\}, \tag{3.4}$$

where Eq (3.2) becomes

$$\mathcal{A}\{u(x, 0)\} = K(u). \tag{3.5}$$

By considering the series solution

$$u = \sum_{n=0}^{\infty} u_n. \tag{3.6}$$

The non-linearity can be obtained as

$$u^m u_x(x,t) = \sum_{i=0}^{\infty} A_n.$$

The value of $A_n$ for the functions $u_i$, $i = 1, 2, 3, \ldots$, is given by [36]

$$A_n = \frac{1}{n!}\frac{d^n}{d\lambda^n}\left[\sum_{k=0}^{n}\lambda^k u_k^m(x,t)\sum_{k=0}^{n}\lambda^k u_{kx}(x,t)\right]_{\lambda=0}. \tag{3.7}$$

Applying an inverse Aboodh transform to above equation, we obtain

$$\begin{aligned}
u_0 &= \mathcal{A}^{-1}\{\frac{1}{v^2}K(u,0)\} = u(x,0).\\
u_1 &= -a\mathcal{A}^{-1}\left\{\frac{1}{v^\alpha}\mathcal{A}\{A_0\}\right\} - b\mathcal{A}^{-1}\left\{\frac{1}{v^\alpha}\mathcal{A}\{u_{0xxx}\}\right\},\\
u_2 &= -a\mathcal{A}^{-1}\left\{\frac{1}{v^\alpha}\mathcal{A}\{A_1\}\right\} - b\mathcal{A}^{-1}\left\{\frac{1}{v^\alpha}\mathcal{A}\{u_{1xxx}\}\right\},\\
u_3 &= -a\mathcal{A}^{-1}\left\{\frac{1}{v^\alpha}\mathcal{A}\{A_2\}\right\} - b\mathcal{A}^{-1}\left\{\frac{1}{v^\alpha}\mathcal{A}\{u_{2xxx}\}\right\},\\
&\vdots\\
u_{n+1} &= -a\mathcal{A}^{-1}\left\{\frac{1}{v^\alpha}\mathcal{A}\{A_n\}\right\} - b\mathcal{A}^{-1}\left\{\frac{1}{v^\alpha}\mathcal{A}\{u_{nxxx}\}\right\}.
\end{aligned} \tag{3.8}$$

The general solution can be written as

$$u(x,t) = u_0(x,t) - a\mathcal{A}^{-1}\left\{\frac{1}{v^\alpha}\mathcal{A}\{A_n\}\right\} - b\mathcal{A}^{-1}\left\{\frac{1}{v^\alpha}\mathcal{A}\{u_{nxxx}\}\right\}. \tag{3.9}$$

## 4. Uniqueness and convergence of the method

The necessary condition that ensures the presence of a unique solution is studied in this section, and the convergence of the solutions is discussed, we follow these theorems applied to the series solutions in [37, 38].

**Theorem 1.** *(Uniqueness theorem) For* $0 < \gamma < 1$*, the solution (3.9) of Eq (3.1) is a unique solution. where*

$$\gamma = \frac{(\ell_1 + \ell_2 + \ell_3)t^{\alpha+1}}{\Gamma(\alpha)}, \tag{4.1}$$

*where* $\ell_1$ *and* $\ell_2$*, are Lipschitz constants,* $0 < \alpha \leq 1$ *and* $\Gamma$ *is the well known Gamma function can be defined as*

$$\Gamma(\alpha) = \int_0^\infty e^{-t}t^{\alpha-1}dt, \quad \mathbb{R} > 0.$$

*Proof.* Define a mapping $\mathscr{D}$: $\mathscr{B}\rightarrow \mathscr{B}$ with $\mathscr{B}$=$(C[J], \|.\|)$ is the Banach space on $J = [0, T]$. We can write Eq (3.9) as

$$u_{n+1} = u(x,0) + \mathscr{A}^{-1}\left\{\frac{1}{v^{\alpha}}\mathscr{A}\Big(\mathscr{H}u_n(x,t) + \mathscr{M}u_n(x,t) + \mathscr{N}u_n(x,t)\Big)\right\},$$

where $\mathscr{H}u = \frac{\partial u}{\partial x}$, $\mathscr{M}u = \frac{\partial^3 u}{\partial x^3}$ and $\mathscr{N}u = u\frac{\partial u}{\partial x}$, and suppose that $\mathscr{H}u$,and $\mathscr{M}u$ are also Lipschitzian with

$$|\mathscr{H}u - \mathscr{H}\bar{u}| < \ell_1 |u - \bar{u}|, \quad |\mathscr{M}u - \mathscr{M}\bar{u}| < \ell_2 |u - \bar{u}|,$$

where $u, \bar{u}$ are the function's distinct values. Now we proceed as follow

$$\begin{aligned}
\|\mathscr{D}u - \mathscr{D}\bar{u}\| &= \max_{t\in J}\left|\mathscr{A}^{-1}\left\{\frac{1}{v^{\alpha}}\mathscr{A}\Big(\mathscr{H}u_n + \mathscr{M}u_n + \mathscr{N}u_n\Big)\right\} - \mathscr{A}^{-1}\left\{\frac{1}{v^{\alpha}}\mathscr{A}\Big(\mathscr{H}\bar{u}_n + \mathscr{M}\bar{u}_n + \mathscr{N}\bar{u}_n\Big)\right\}\right| \\
&\leq \max_{t\in J}\left|\mathscr{A}^{-1}\left\{\frac{1}{v^{\alpha}}\mathscr{A}\Big(\mathscr{H}u_n - \mathscr{H}\bar{u}\Big)\right\} + \mathscr{A}^{-1}\left\{\frac{1}{v^{\alpha}}\mathscr{A}\Big(\mathscr{M}u - \mathscr{M}\bar{u}\Big)\right\}\right. \\
&\quad \left. + \mathscr{A}^{-1}\left\{\frac{1}{v^{\alpha}}\mathscr{A}\Big(\mathscr{N}u - \mathscr{N}\bar{u}\Big)\right\}\right| \\
&\leq \max_{t\in J}\left|\ell_1\mathscr{A}^{-1}\left\{\frac{1}{v^{\alpha}}\mathscr{A}\Big(u - \bar{u}\Big)\right\} + \ell_2\mathscr{A}^{-1}\left\{\frac{1}{v^{\alpha}}\mathscr{A}\Big(u - \bar{u}\Big)\right\} + \ell_3\mathscr{A}^{-1}\left\{\frac{1}{v^{\alpha}}\mathscr{A}\Big(\mathscr{N}u - \bar{u}\Big)\right\}\right| \\
&\leq \max_{t\in J}(\ell_1 + \ell_2 + \ell_3)\left|\mathscr{A}^{-1}\left\{\frac{1}{v^{\alpha}}\mathscr{A}\Big(u - \bar{u}\Big)\right\}\right| \\
&= \frac{(\ell_1 + \ell_2 + \ell_3)t^{(\alpha-1)}}{\Gamma(\alpha)}\|u - \bar{u}\|.
\end{aligned}$$

The mapping is contraction under the condition $0 < \gamma < 1$. As a result of the Banach fixed point theorem for contraction, Eq (3.1) has a unique solution. □

Next, we discuss convergence analysis of the problems.

**Theorem 2.** *(Convergence theorem) The solution of Eq (3.1) in general form will be convergence.*

*Proof.* The Banach space of all continuous functions on the interval $J$ with the norm $\|u(x,t)\|$=$\max_{t\in J}\|u(x,t)\|$ is denoted as $(C[J], \|.\|)$. Define the $\{\mathscr{S}n\}$ sequence of partial sums that is $\mathscr{S}_n$=$\sum_{j=0}^{n}$. With $n \geq m$, let $\mathscr{S}_n$ and $\mathscr{S}_m$ be arbitrary partial sums. In this Banach space, we will show that $\mathscr{S}_n$ is a Cauchy sequence. This can obtained by employing a new formulation of Adomian polynomials.

$$P(\mathscr{S}_n) = \bar{A}_n + \sum_{r1=0}^{n-1} \bar{A}_{r_1}, \quad Q(\mathscr{S}_n) = \bar{A}_n + \sum_{r2=0}^{n-1} \bar{A}_{r_2}.$$

Now

$$\begin{aligned}
\|\mathscr{S}_n - \mathscr{S}_m\| &= \left| \sum_{j=0}^{n} u_j - \sum_{k=0}^{m} u_k \right| = \max_{t\in J} \left| \sum_{j=m+1}^{n} u_j \right| \\
&\leq \max_{t\in J} \left| \mathcal{A}^{-1} \left\{ \frac{1}{v^\alpha} \mathcal{A}\Big( \sum_{j=m+1}^{n} \mathscr{H}(u_{j-1}) \Big) \right\} + \mathcal{A}^{-1} \left\{ \frac{1}{v^\alpha} \mathcal{A}\Big( \sum_{j=m+1}^{n} \mathscr{M}(u_{j-1}) \Big) \right\} \right. \\
&\quad \left. + \mathcal{A}^{-1} \left\{ \frac{1}{v^\alpha} \mathcal{A}\Big( \sum_{j=m+1}^{n} (A_{j-1}) \Big) \right\} \right| \\
&= \max_{t\in J} \left| \mathcal{A}^{-1} \left\{ \frac{1}{v^\alpha} \mathcal{A}\Big( \sum_{j=m}^{n-1} \mathscr{H}(u_j) \Big) \right\} + \mathcal{A}^{-1} \left\{ \frac{1}{v^\alpha} \mathcal{A}\Big( \sum_{j=m}^{n-1} \mathscr{M}(u_j) \Big) \right\} + \mathcal{A}^{-1} \left\{ \frac{1}{v^\alpha} \mathcal{A}\Big( \sum_{j=m}^{n-1} (A_j) \Big) \right\} \right| \\
&\leq \max_{t\in J} \left| \mathcal{A}^{-1} \left\{ \frac{1}{v^\alpha} \mathcal{A}\Big( \sum_{j=m}^{n-1} \mathscr{H}(\mathscr{S}_{n-1}) - \mathscr{H}(\mathscr{S}_{m-1}) \Big) \right\} + \mathcal{A}^{-1} \left\{ \frac{1}{v^\alpha} \mathcal{A}\Big( \sum_{j=m}^{n-1} \mathscr{M}(\mathscr{S}_{n-1}) - \mathscr{M}(\mathscr{S}_{m-1}) \Big) \right\} \right. \\
&\quad \left. + \mathcal{A}^{-1} \left\{ \frac{1}{v^\alpha} \mathcal{A}\Big( \sum_{j=m}^{n-1} \mathscr{N}(\mathscr{S}_{n-1}) - \mathscr{N}(\mathscr{S}_{m-1}) \Big) \right\} \right| \\
&\leq \ell_1 \max_{t\in J} \left| \mathcal{A}^{-1} \left\{ \frac{1}{v^\alpha} \mathcal{A}\Big( (\mathscr{S}_{n-1}) - (\mathscr{S}_{m-1}) \Big) \right\} \right| + \ell_2 \max_{t\in J} \left| \mathcal{A}^{-1} \left\{ \frac{1}{v^\alpha} \mathcal{A}\Big( (\mathscr{S}_{n-1}) - (\mathscr{S}_{m-1}) \Big) \right\} \right| \\
&\quad + \ell_3 \max_{t\in J} \left| \mathcal{A}^{-1} \left\{ \frac{1}{v^\alpha} \mathcal{A}\Big( (\mathscr{S}_{n-1}) - (\mathscr{S}_{m-1}) \Big) \right\} \right| = \frac{(\ell_1 + \ell_2 + \ell_3) t^{\alpha-1}}{\Gamma(\alpha)} \|\mathscr{S}_{n-1} - \mathscr{S}_{m-1}\|.
\end{aligned}$$

Choosing $n = m + 1$ then

$$\|\mathscr{S}_{m+1} - \mathscr{S}_m\| \leq \gamma \|\mathscr{S}_m - \mathscr{S}_{m-1}\| \leq \gamma^2 \|\mathscr{S}_{m-1} - \mathscr{S}_{m-2}\| \leq \cdots\cdots \leq \gamma^m \|\mathscr{S}_1 - \mathscr{S}_0\|,$$

with $\gamma = \frac{(\ell_1+\ell_2+\ell_3)t^{\alpha-1}}{\Gamma(\alpha)}$, by using the following triangular inequality

$$\begin{aligned}
\|\mathscr{S}_n - \mathscr{S}_m\| &\leq \|\mathscr{S}_m - \mathscr{S}_{m+1}\| \leq \|\mathscr{S}_{m+1} - \mathscr{S}_{m+2}\| \leq \cdots\cdots \leq \gamma^m \|\mathscr{S}_1 - \mathscr{S}_0\| \\
&\leq \left(\gamma^m + \gamma^{m+1} + \cdots + \gamma^n\right) \|\mathscr{S}_1 - \mathscr{S}_0\| \\
&\leq \gamma^m \left(1 + \gamma + \gamma^2 + \cdots + \gamma^{n-m-1}\right) \|\mathscr{S}_1 - \mathscr{S}_0\| \\
&\leq \gamma^m \left(\frac{1 - \gamma^{n-m}}{1 - \gamma}\right) \|u_1\|.
\end{aligned}$$

Now by definition $0 < \gamma < 1$, we have $1 - \gamma^{n-m} < 1$, thus we have

$$\|\mathscr{S}_n - \mathscr{S}_m\| \leq \frac{\gamma^m}{1-\gamma} \max_{t\in J} \|u_1\|, \tag{4.2}$$

and also as $|u| < \infty$ ($u$ is bounded), therefore, $\|\mathscr{S}_n - \mathscr{S}_m\| \to 0$, hence $\mathscr{S}_n$ is a Cauchy sequence in the Banach space $\mathscr{B}$, hence $\sum_{j=0}^{n} u_j$ is convergent. □

## 5. Applications of ADM

In this section, we consider two specific examples of time-fractional Korteweg-de Vries (TF-KdV) and time-fractional modified Korteweg-de Vries (TF-mKdV) equations in the form of Eq (1.1) with some initial conditions and apply ADM to find their approximate solutions.

Next we consider two examples one for time-fractional order KdV and the other for time-fractional mKdV and use the propose method (ADM) to obtain an approximate solution.

**Example 1.** *For $m = 1$ in Eq (3.1) we can take the following TF-KdV in Caputo's form [39]*

$$^{c}D_t^{\alpha} u + au\frac{\partial u}{\partial x} + b\frac{\partial^3 u}{\partial x^3} = 0, \quad 0 < \alpha \leq 1, \tag{5.1}$$

*with initial condition of the form*

$$u_0 = u(x, 0) = A\,\mathrm{sech}^2(kx). \tag{5.2}$$

*The exact solution for $\alpha = 1$ of Eq (5.1) [39]*

$$u = A\ \mathrm{sech}^2(kx - 4k^3 bt), \tag{5.3}$$

where $A = \frac{12k^2 b}{a}$ is amplitude and $4bk^3$ is the speed of the wave function. Applying ADM to Eq (5.1) and decomposing the non-linear term $uu_x$ by using the Adomian formula (3.7), we obtain the following Adomian polynomials

$$A_0 = u_0 u_{0x}, \quad A_1 = u_0 u_{1x} + u_1 u_{0x}, \quad A_2 = u_0 u_{2x} + u_1 u_{1x} + u_2 u_{0x}, \quad A_3 = u_0 u_{3x} + u_1 u_{2x} + u_3 u_{0x} + u_2 u_{1x},$$

putting the above values in Eq (3.8) with assumption $h_0(x) = u_0(x, 0)$ with $h_1(x) = h_2(x) = h_3(x) = 0$, we obtain the following single soliton solution for the TF-KdV Eq (5.1) in the form

$$u_0 = h_0(x), \quad u_1 = \frac{t^{\alpha}}{\Gamma(\alpha+1)} f_1(x), \quad u_2 = -\frac{t^{2\alpha}}{\Gamma(2\alpha+1)} f_2(x), \quad u_3 = \frac{t^{3\alpha}}{\Gamma(3\alpha+1)} f_3(x),$$

where

$$\begin{aligned} f_1(x) &= ah_0 h_{0x} + bh_{0xxx}, \quad f_2(x) = a(h_0 f_{1x} + 2h_0 f_1 h_{0x}) + bf_{1xxx}, \\ f_3(x) &= a\left[h_0 f_{2x} + 2h_0 f_2 h_{0x} + \frac{\Gamma(2\alpha+1)}{\Gamma(\alpha+1)}(2h_0 f_1 f_{1x} h_{0x} + f_1 h_{0x})\right] + bf_{2xxx}. \end{aligned}$$

The final solution in the series form up to $O(4)$ is given by

$$U(x,t) = h_0(x) + \frac{t^{\alpha}}{\Gamma(\alpha+1)} f_1(x) - \frac{t^{2\alpha}}{\Gamma(2\alpha+1)} f_2(x) + \frac{t^{3\alpha}}{\Gamma(3\alpha+1)} f_3(x). \tag{5.4}$$

For $\alpha = 1$, we obtain

$$u(x,t) = \frac{12k^2b}{a}\ \mathrm{sech}^2(kx - 4k^3bt).$$

The ADM solution for different $\alpha$ are reported in Table 1, by considering $k = 0.1, a = 2, b = 0.2, t = 1$.

Figure 1(a,b) displays the zeroth and higher order solitary wave solutions (5.3) and (5.4) versus the space variable $x$ respectively for time-fractional KdV Eq (5.1) for small time of $t$. It infers that at $t > 0$ the higher order solitary wave solution is significantly modified. The wave three-dimensional profiles for solutions (5.3) and (5.4) in Figure 1(c,d) also reveal that variations in temporal variables affect the amplitude and spatial extensions of the higher order wave solutions. We have plotted the approximate solution (5.3) against $t$ at $x = 0.5$ and 1 respectively, with variation in the time-fractional index $\alpha$ [see Figure 2(a,b)]. A degree of enhancement in $\alpha$ reduces the spatial width of the solitary waves. Thus, the time-fractional index leads to a reduction in the wave dispersion that in turn localises the wave profile. The effect of the non-linearity coefficient "a" is shown in Figure 3(a). We see that the amplitude of the solitary wave decreases regularly when the values of the non-linearity coefficient are increasing. This definitely occurs for wave equations because the non-linearity coefficient has an inverse proportionality with the solitary wave amplitude. On the other hand, the wave amplitude is gradually increasing with the increasing values of the dispersion coefficient "b" in Figure 3(b). The dispersive coefficient is proportional to the amplitude of a solitary wave. We have depicted the higher order solution (5.4) for the TF-KdV Eq (5.1), verses $x$ at time $t = 3$ (solid curve), at 3.5 (dashed curve), and at 4 (dotted curve) [see Figure 4(a)]. Obviously, the enhancement in $t$ gives rise to the pulse amplitude while increasing the spatial width. Moreover, the pulse shape solutions suffer from oscillations for $t > 0$. The wave solution (5.4) presented in Figure 4(b) at different values of the temporal index ($\alpha$) reveals strengthening of the wave with wider spatial extension at large $\alpha$. One can see that the solitary wave solutions for the TF-KdV equation are observed. By employing an Aboodh decomposition (ADM) technique and with the addition of $t$ the Caputo operator for the solitary excitations are derived in Eq (5.4). Importantly, the wave solution significantly changes in time. The large amplitude electrostatic excitations in the auroral zone [27], associated with the intensified electric field. These may be described by the solutions (5.3) and (5.4) for the TF-KdV equation of Exp.1. Our results obtained in this paper are so important because the waves produced by the solutions of the TF-KdV may have very high amplitudes. The amplitudes of these waves can be reduced by using the fractional order of the wave equations. In other words, by taking the fractional order of the time derivative term, a better analysis of the waves can be achieved.

**Table 1.** Evaluation between approximate ($U(x,t)$) versus an exact solution (u(x,t) for different values a=0.2, b=0.4, k=0.1, $-10 \leq x \leq 10$ and $0 \leq t \leq 1$ Exp.1.

| t | $U(\alpha = 0.3)$ | $U(\alpha = 0.5)$ | $U(\alpha = 0.7)$ | $U(\alpha = 0.9)$ | $U(\alpha = 1)$ | Exact | MAE |
|---|---|---|---|---|---|---|---|
| | | | | x=-10 | | | |
| 0.00 | 0.0050869 | 0.0050869 | 0.0050869 | 0.0050869 | 0.0050869 | 0.0050869 | |
| 0.25 | 0.0050056 | 0.0050276 | 0.0050447 | 0.0050575 | 0.0050625 | 0.0050634 | |
| 0.50 | 0.0049834 | 0.0049994 | 0.0050155 | 0.0050302 | 0.0050367 | 0.0050400 | 4.0619E-05 |
| 0.75 | 0.0049673 | 0.0049763 | 0.0049888 | 0.0050025 | 0.0050093 | 0.0050167 | |
| 1.00 | 0.0049542 | 0.0049559 | 0.0049633 | 0.0049742 | 0.0049803 | 0.0049935 | |
| | | | | x=-5 | | | |
| 0.00 | 0.030238 | 0.030238 | 0.030238 | 0.030238 | 0.030238 | 0.030238 | |
| 0.25 | 0.029905 | 0.029984 | 0.030052 | 0.030105 | 0.030127 | 0.030128 | |
| 0.50 | 0.029825 | 0.029877 | 0.029933 | 0.029989 | 0.030015 | 0.030018 | 1.2525E-04 |
| 0.75 | 0.02977 | 0.029793 | 0.029831 | 0.0050025 | 0.029902 | 0.029908 | |
| 1.00 | 0.029726 | 0.029722 | 0.029737 | 0.0049742 | 0.029787 | 0.029798 | |
| | | | | x=0 | | | |
| 0.00 | 0.0720000 | 0.0720000 | 0.0720000 | 0.0720000 | 0.0720000 | 0.0720000 | |
| 0.25 | 0.071994 | 0.071997 | 0.071998 | 0.071999 | 0.0720000 | 0.0720000 | |
| 0.50 | 0.07199 | 0.071993 | 0.071996 | 0.071998 | 0.0719987 | 0.0719987 | 6.2213E-06 |
| 0.75 | 0.071988 | 0.07199 | 0.071993 | 0.071995 | 0.071996 | 0.071996 | |
| 1.00 | 0.071985 | 0.071987 | 0.071989 | 0.071992 | 0.071993 | 0.071993 | |
| | | | | x=5 | | | |
| 0.00 | 0.030238 | 0.030238 | 0.030238 | 0.030238 | 0.030238 | 0.030238 | |
| 0.25 | 0.030555 | 0.030483 | 0.03042 | 0.030369 | 0.030348 | 0.030349 | |
| 0.50 | 0.030625 | 0.030582 | 00.030532 | 0.030481 | 0.030457 | 0.03046 | 1.0040E-04 |
| 0.75 | 0.030673 | 0.030657 | 0.030626 | 0.030587 | 0.030565 | 0.030571 | |
| 1.00 | 0.030711 | 0.030719 | 0.03071 | 0.030687 | 0.030671 | 0.030682 | |
| | | | | x=10 | | | |
| 0.00 | 0.0050869 | 0.0050869 | 0.0050869 | 0.0050869 | 0.0050869 | 0.0050869 | |
| 0.25 | 0.005144 | 0.0051338 | 0.0050447 | 0.0051233 | 0.0051096 | 0.0051105 | |
| 0.50 | 0.0051538 | 0.0051496 | 0.0050155 | 0.0051431 | 0.0051308 | 0.0051341 | 1.4575E-05 |
| 0.75 | 0.0051598 | 0.0051603 | 0.0049888 | 0.0051583 | 0.0051505 | 0.0051579 | |
| 1.00 | 0.0051641 | 0.0051684 | 0.0049633 | 0.0051706 | 0.0051687 | 0.0051819 | |

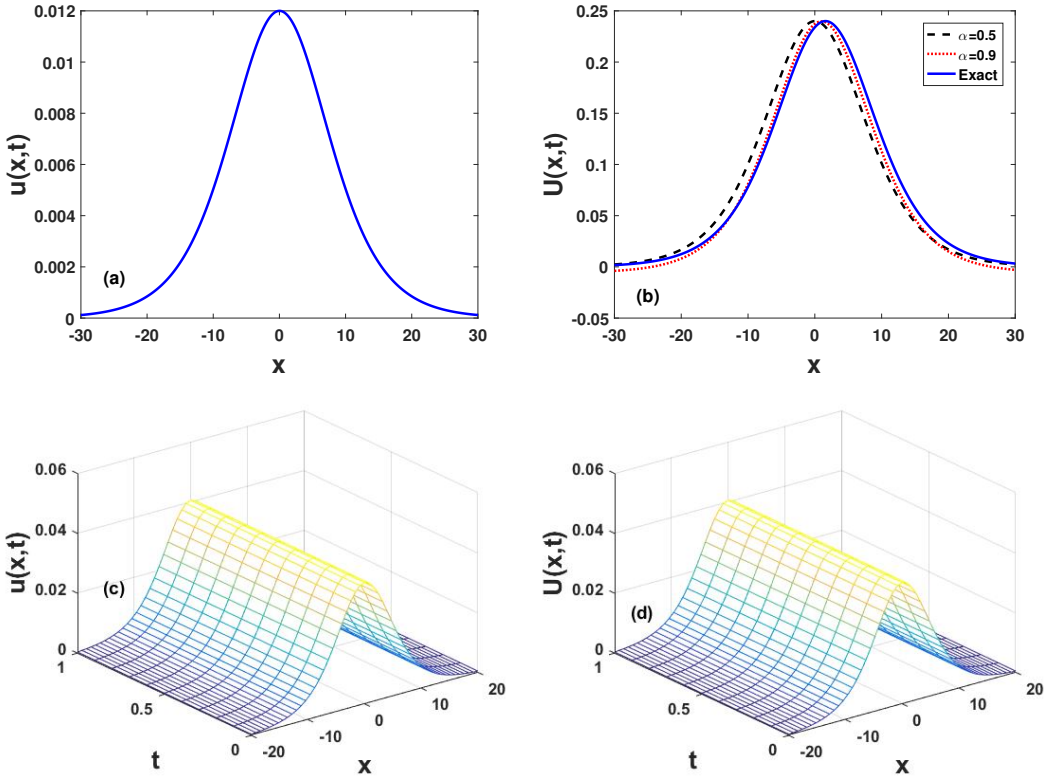


**Figure 1.** In the top panel, (a) shows exact solution of Eq (5.3), while (b) shows comparison of approximate (ADM) and exact solution Eq (5.4) $k = 0.1, a = 0.2, b = 0.4$, for small time $t = 0.2$. The bottom panel (c,d) are corresponding surface 3D plots for both solutions against the temporal variables $(x, t)$ with parameters ($\alpha = 1$ for exact, and 0.7, for the approximate solution, with fixed $k = 0.1, a = 2, b = 0.2, t = 1$).

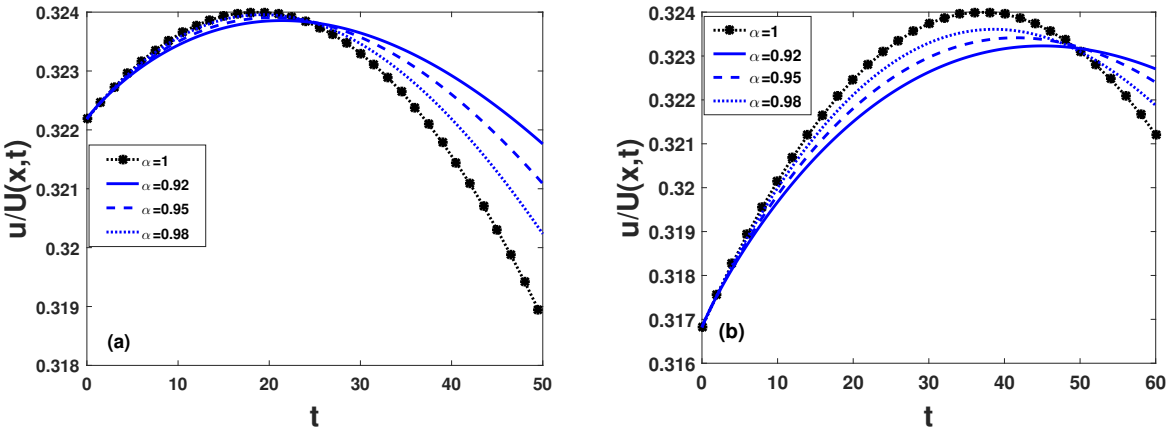


**Figure 2.** The above plots show the dispersive behaviours of the solitary waves by varying time and the fractional order $\alpha$ with fixed special variable (a) $x = 0.5$ and (b) $x = 1$ of the exact ($\alpha = 1$ star black) solution Eq (5.3) and approximate ($\alpha < 1$ blue) solution Eq (5.4) respectively.

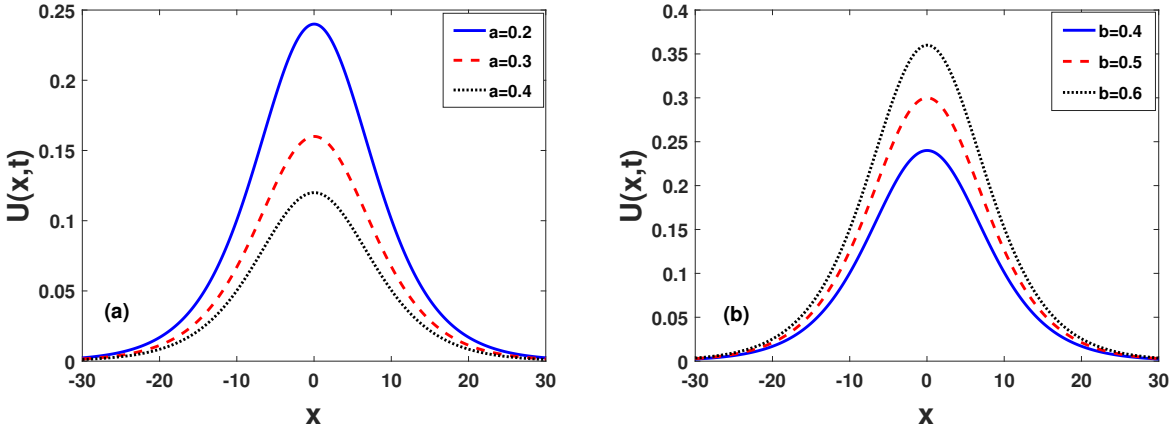


**Figure 3.** Solitary waves profiles for different values of (a) the non-linearity coefficient "a" with b=0.4 and (b) the dispersive coefficient "b" with a=0.2, when the wave number k=0.1, the fractional index $\alpha = 0.5$ and t=0.5 of Eq (5.4).

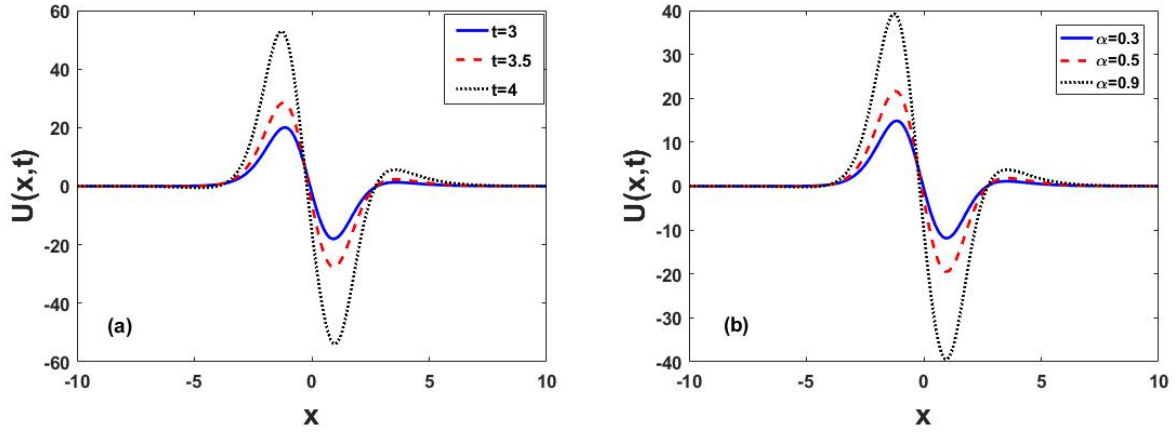


**Figure 4.** Plots of the approximate solution for (a) different values of t with $\alpha = 0.9$ (b) different values of $\alpha$ for larger time and the other parameters are $a = 0.9, k = 0.5, b = 0.9$ of Eq (5.4).

**Example 2.** *For $m = 2, a = 6, b = 1$, the modified time-fractional KdV [26] in Caputo's sense is given by*

$$ {}^{C}D_t^{\alpha} v + 6\, v^2 \frac{\partial v}{\partial x} + \frac{\partial^3 v}{\partial x^3} = 0, \quad 0 < \alpha \leq 1, \tag{5.5} $$

with

$$ v_0 = v(x, 0) = \sqrt{c}\, \mathrm{sech}^2(k + \sqrt{c}x). \tag{5.6} $$

When $\alpha = 1$, Eq (5.5) gives [26]

$$ v(x, t) = \sqrt{c}\ \mathrm{sech}(k + \sqrt{c}x - ct). \tag{5.7} $$

Applying the ADM to Eq (5.5) and decompose the non-linear term $v^2v_x$ in Eq (5.5) by using the Adomian formula (3.7), we obtain

$$A_0 = v_0^2v_{0x}, \quad A_1 = v_0^2v_{1x} + v_1^2v_{0x}, \quad A_2 = v_0^2v_{2x} + v_1^2v_{1x} + v_2^2v_{0x}, \quad A_3 = v_0^2v_{3x} + v_1^2v_{2x} + v_3^2v_{0x} + v_2^2v_{1x}.$$

Putting $a = 6$ and $b = 1$ in Eq (3.8) and assume that $g_0(x) = v(x, 0)$ with $g_1(x) = g_2(x) = g_3(x)$, we obtain

$$v_0 = g_0(x), \quad v_1 = \frac{t^\alpha}{\Gamma(\alpha+1)}q_1(x), \quad v_2 = -\frac{t^{2\alpha}}{\Gamma(2\alpha+1)}q_2(x), \quad v_3 = \frac{t^{3\alpha}}{\Gamma(3\alpha+1)}q_3(x),$$

where

$$\begin{aligned} q_1(x) &= 6g_0^2g_{0x} + g_{0xxx}, \quad q_2(x) = 6(g_0^2q_{1x} + 2g_0q_1g_{0x}) + q_{1xxx}, \\ q_3(x) &= 6\left[g_0^2q_{2x} + 2g_0q_2g_{0x} + \frac{\Gamma(2\alpha+1)}{\Gamma(\alpha+1)}(2g_0q_1q_{1x}g_{0x} + q_1^2g_{0x})\right] + q_{2xxx}. \end{aligned}$$

The solution up to $O(4)$ can be written as

$$V(x,t) = g_0(x) + \frac{t^\alpha}{\Gamma(\alpha+1)}q_1(x) - \frac{t^{2\alpha}}{\Gamma(2\alpha+1)}q_2(x) + \frac{t^{3\alpha}}{\Gamma(3\alpha+1)}q_3(x). \tag{5.8}$$

For $\alpha = 1$ we found the following exact solution

$$v(x,t) = \sqrt{c}\ \mathrm{sech}(k + \sqrt{c}x - ct).$$

We have displayed the zeroth (higher) order solitary wave solutions (5.7) and (5.8) in Figure 5(a,b) respectively, for the modified time-fractional KdV Eq (5.5) verses x for small t. Notice that the wave solution of the TF-mKdV equation suffers only a relatively modest steeping effect with a reduction in the wave dispersion. Moreover, at $t > 0$ the higher-order solution illustrates noticeable modifications in the wave profiles. The three dimensional profiles Figure 5(c,d) for the time fractional (exact and approximate) solutions also confirm that both the solutions are quite similar. Figure 6(a,b) display the solution (5.8) at $x = 0.5$ and 1 respectively with variation in $\alpha$. Contrary to the TF-KdV solution, the wave solution for TF-mKdV admits reduced wave dispersion at $t > 0$. We observed that, the dispersive approximate solution ($\alpha < 1$ the blue curves) approaching to the exact solution ($\alpha = 1$, black curve) when then $\alpha$ values are approaching to 1. In Figure 7(a), we depicted the approximate (ADM) solution against the special variable x by changing the wave speed "c=0.1 (solid curve), 0.2 (dashed curve), and 0.3 (dotted curve)". We observed that when the speed "c" is increasing, the wave amplitude is increasing while its width is decreasing, which shows that the amplitude is directly proportional to the wave speed while the width of the wave is inversely related to the wave speed. Similarly, in Figure 7(b), we displayed the approximate solution against "x" by changing the wave number "k=0.5 (solid curve), 1 (dashed curve), and 1.5 (dotted curve)". We see that, for different values of the wave number and equal amplitudes, wave profiles are obtained. The wave solution (5.5) for TF-mKdV in Figure 8(a) shows at different times that the solitary waves suffer from oscillation due to the external perturbations. It also shows that the solitary solution for the TF-mKdV is relatively less stable against the perturbations. Moreover, the increase in $t$ and $\alpha$ modify the amplitude and width of the wave. Variation of the $\alpha$ value for the approximate solution is shown in Figure 8(b) against $x$. We observed from the Figure 8(a,b) when the temporal variable (t) and the fractional order $\alpha$ increasing the amplitudes of the wave profile getting larger values.

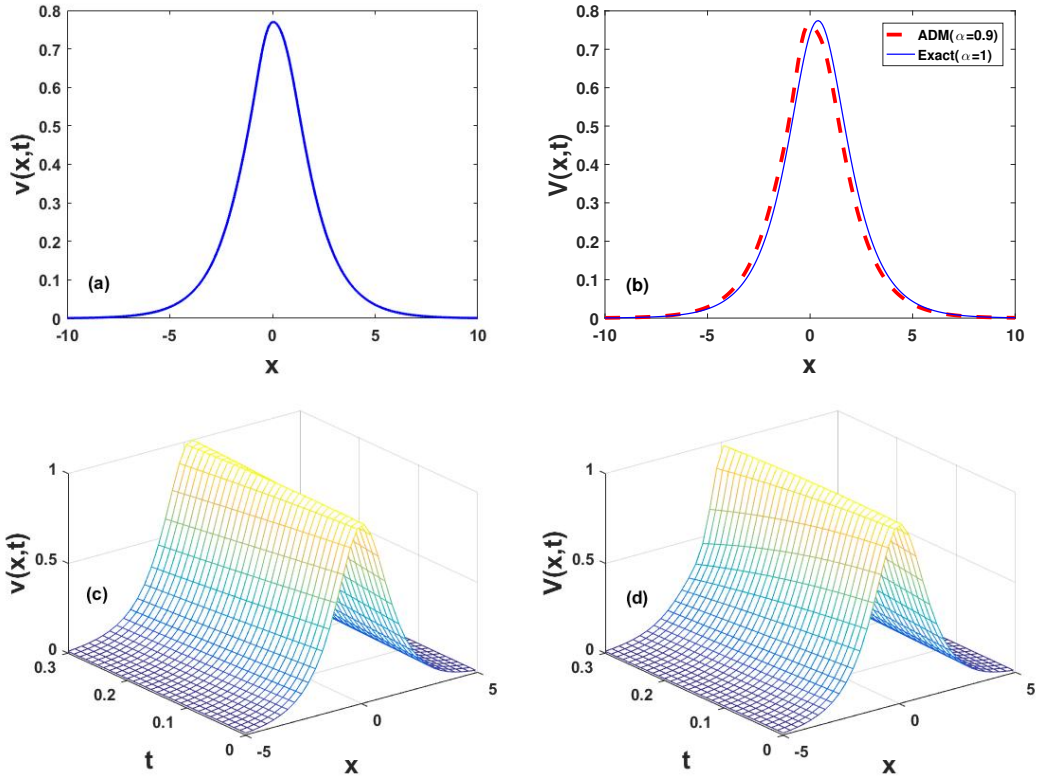


**Figure 5.** In the top panel, (a) shows exact solution for Eq (5.7) while (b) shows a comparison of exact and approximate solution (ADM) of Eq (5.8). The bottom panel (c,d) are the corresponding surface 3D plots against the temporal variables $(x, t)$ with parameters ($\alpha = 1$ for exact, and 0.7, for the approximate solution, with fixed $k = 0, c = 1, t = 0.2$).

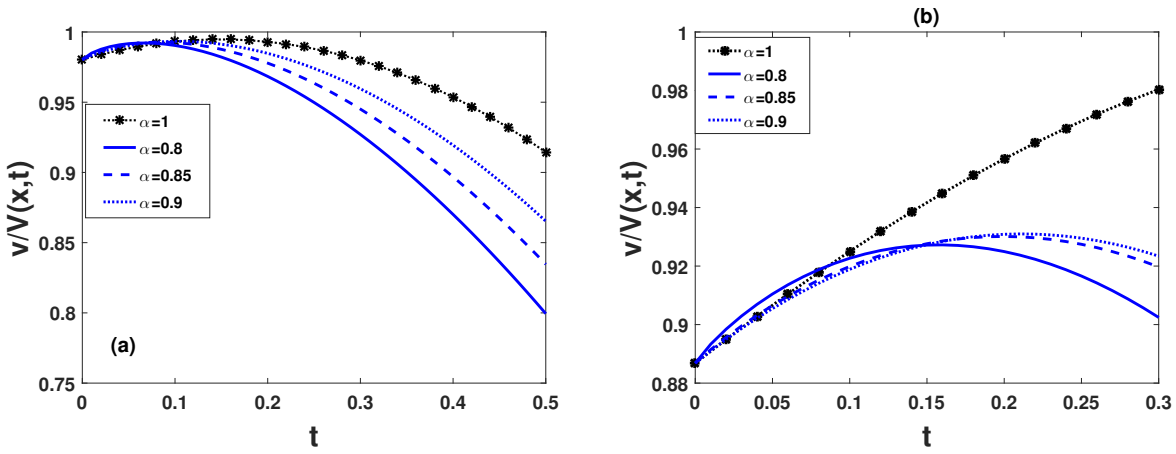


**Figure 6.** Dispersive behaviours of the solitary waves by varying time and the fractional order $\alpha$ with fixed special variable (a) $x = 0.5$ and (b) $x = 1$ for exact ($\alpha = 1$ stars blue curve of Eq (5.7)) and approximate ($\alpha < 1$ blue curves Eq (5.8)) respectively.

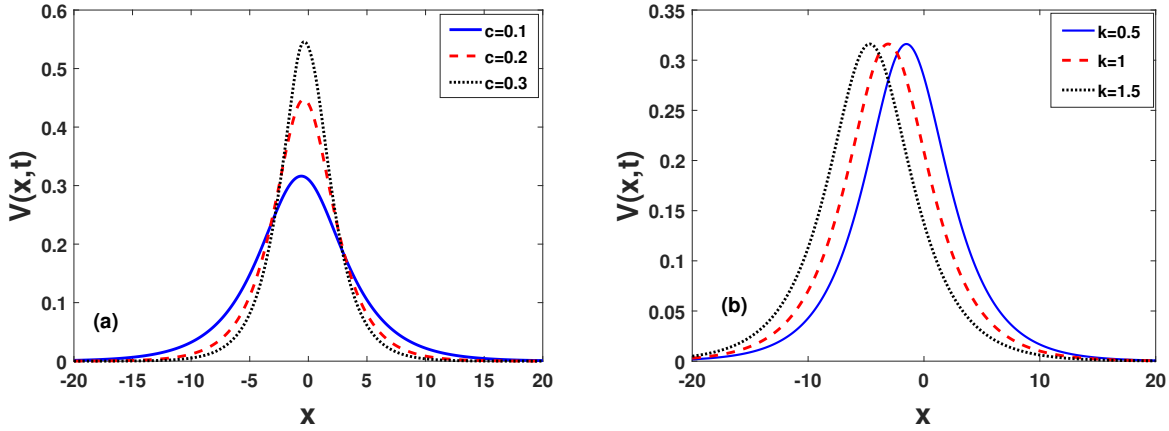


**Figure 7.** Solitary waves profiles for different values of (a) the speed "c" with k=0.5 and (b) the wave number "k", with c=0.2 when the fractional index $\alpha = 0.7$ and t=0.5 of Eq (5.8).

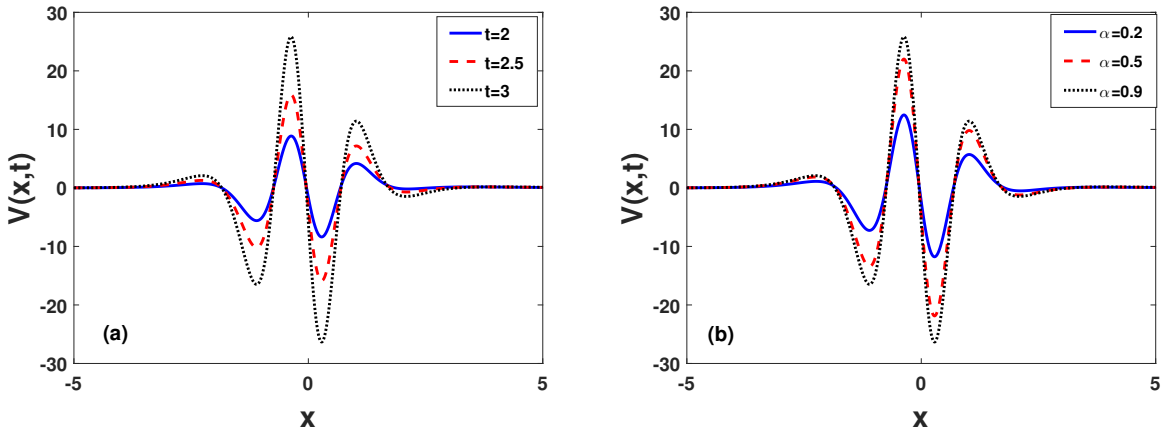


**Figure 8.** Plots of the approximate solution for (a) different values of $t$ with $\alpha = 0.9$ (b) different values of $\alpha$ for larger time values and other parameters are $c = 0.6, k = 0$ of Eq (5.8).

The mean absolute error (MAE) is a statistic that calculates the variance in errors amongst matching interpretations representing identical singularities. The relationships between an exact and an approximate solution, future time against beginning time, and one measuring method versus another quantity technique are all examples of $y$ versus $x$. The MAE can be computed as

$$MAE = \frac{1}{n}\sum_{i=1}^{n}|y_i - x_i|, \tag{5.9}$$

where, $x_i$ is the expected value and $y_i$ is the real value of the system. The following figures are obtained from the error analysis in the Tables 1–4.

**Table 2.** Comparison between the approximate solution ($V(x,t)$), versus an exact solution ($v(x,t)$) for $-10 \leq x \leq 10$ and $0 \leq t \leq 1$ with k=0.5 and c=0.82 of Exp.2.

| t | $V(\alpha = 0.3)$ | $V(\alpha = 0.5)$ | $V(\alpha = 0.7)$ | $V(\alpha = 0.9)$ | $V(\alpha = 1)$ | Exact | MAE |
|---|---|---|---|---|---|---|---|
| | | | | x=-10 | | | |
| 0.00 | 0.010216 | 0.010216 | 0.010216 | 0.010216 | 0.010216 | 0.010216 | |
| 0.25 | 0.0095819 | 0.00972 | 0.0098439 | 0.0099468 | 0.0099898 | 0.0097175 | |
| 0.50 | 0.0094455 | 0.0095258 | 0.0096209 | 0.0097203 | 0.0097689 | 0.0092437 | 3.6330E-04 |
| 0.75 | 0.0093537 | 0.0093809 | 0.0094359 | 0.0095107 | 0.0095529 | 0.008793 | |
| 1.00 | 0.0092825 | 0.0092616 | 0.0092729 | 0.0093128 | 0.0093417 | 0.0083642 | |
| | | | | x=-5 | | | |
| 0.00 | 0.094515 | 0.094515 | 0.094515 | 0.094515 | 0.094515 | 0.094515 | |
| 0.25 | 0.088823 | 0.090001 | 0.091122 | 0.092066 | 0.09246 | 0.090002 | |
| 0.50 | 0.087702 | 0.088282 | 0.089091 | 0.08999 | 0.090436 | 0.085696 | 3.5E-03 |
| 0.75 | 0.086993 | 0.087053 | 0.087436 | 0.08807 | 0.088455 | 0.081589 | |
| 1.00 | 0.086476 | 0.08609 | 0.086022 | 0.086289 | 0.08653 | 0.077671 | |
| | | | | x=0 | | | |
| 0.00 | 0.447210 | 0.447210 | 0.447210 | 0.447210 | 0.447210 | 0.447210 | |
| 0.25 | 0.445160 | 0.446220 | 0.446770 | 0.447030 | 0.44710 | 0.446660 | |
| 0.50 | 0.444000 | 0.445150 | 0.446010 | 0.446560 | 0.446740 | 0.444990 | 1.46E-03 |
| 0.75 | 0.443020 | 0.444030 | 0.445030 | 0.445830 | 0.446130 | 0.442230 | |
| 1.00 | 0.442140 | 0.442860 | 0.443860 | 0.444830 | 0.445250 | 0.438420 | |
| | | | | x=5 | | | |
| 0.00 | 0.094515 | 0.094515 | 0.094515 | 0.094515 | 0.094515 | 0.094515 | |
| 0.25 | 0.099243 | 0.099243 | 0.099243 | 0.099243 | 0.099243 | 0.030349 | |
| 0.50 | 0.104190 | 0.104190 | 0.10419 | 0.030481 | 0.10419 | 0.104190 | 4.446E-03 |
| 0.75 | 0.109380 | 0.109380 | 0.109380 | 0.0305870 | 0.10938 | 0.109380 | |
| 1.00 | 0.114800 | 0.114800 | 0.114800 | 0.0306870 | 0.1148 | 0.030682 | |
| | | | | x=10 | | | |
| 0.00 | 0.010216 | 0.010216 | 0.010216 | 0.010216 | 0.010216 | 0.010216 | |
| 0.25 | 0.010928 | 0.010752 | 0.010606 | 0.010492 | 0.010447 | 0.010739 | |
| 0.50 | 0.011106 | 0.01117 | 0.011083 | 0.010978 | 0.010683 | 0.01129 | 4.3146E-04 |
| 0.75 | 0.01133 | 0.011332 | 0.011289 | 0.011215 | 0.010924 | 0.011868 | |
| 1.00 | 0.114800 | 0.11480 | 0.114800 | 0.030687 | 0.011171 | 0.012477 | |

**Table 3.** Comparison of exact solution (u(x,t)) with approximate (U(x,t)) solution for $\alpha$ = 0.5, a=0.2, b=0.4, and k=1 of Exp.1.

| $x$ | t | $\xi$=$kx - 4bk^3t$ | Exact solution | ADM Solution | Error |
|---|---|---|---|---|---|
| -50 | 0.00 | -49.9434 | -0.35995 | -0.35995 | $2.5009\times10^{-08}$ |
| -40 | 0.25 | -39.6454 | -0.35965 | -0.35965 | $1.9820\times10^{-07}$ |
| -30 | 0.50 | -29.6453 | -0.35745 | -0.35746 | $2.1868\times10^{-06}$ |
| -20 | 0.75 | -19.6423 | -0.34165 | -0.34170 | $5.1926\times10^{-05}$ |
| ... | ... | ... | ... | ... | ... |
| ... | ... | ... | ... | ... | ... |
| ... | ... | ... | ... | ... | ... |
| ... | ... | ... | ... | ... | ... |
| ... | ... | ... | ... | ... | ... |
| 20 | 0.25 | 20.3634 | 0.11987 | 0.11988 | $-1.6363\times10^{-05}$ |
| 30 | 0.50 | 30.3653 | 0.12000 | 0.12000 | $-3.3767\times10^{-07}$ |
| 40 | 0.75 | 40.3634 | 0.12000 | 0.12000 | $-6.2851\times10^{-09}$ |
| 50 | 1.00 | 50.3643 | 0.12000 | 0.12000 | $-1.1537\times10^{-10}$ |

**Table 4.** Comparison of exact (v(x,t)) solution with approximate (V(x,t) solution for k=0.5, and c=0.82 of Exp.2.

| $x$ | t | $\xi$=$k + \sqrt{c}x - ct$ | Exact solution | ADM Solution | Error |
|---|---|---|---|---|---|
| -50 | 0.00 | -45.5969 | -0.35995 | -0.35995 | $-2.8783\times10^{-07}$ |
| -40 | 0.25 | -36.5415 | -0.35966 | -0.35966 | $-2.1145\times10^{-06}$ |
| -30 | 0.50 | -27.4862 | -0.35751 | -0.35750 | $-1.4960\times10^{-05}$ |
| -20 | 0.75 | -18.4308 | -0.34207 | -0.34199 | $-7.7286\times10^{-05}$ |
| ... | ... | ... | ... | ... | ... |
| ... | ... | ... | ... | ... | ... |
| ... | ... | ... | ... | ... | ... |
| ... | ... | ... | ... | ... | ... |
| ... | ... | ... | ... | ... | ... |
| 20 | 0.25 | 17.7908 | 0.11986 | 0.11987 | $-1.3770\times10^{-05}$ |
| 30 | 0.50 | 26.8462 | 0.12000 | 0.12000 | $-2.8188\times10^{-07}$ |
| 40 | 0.75 | 35.9015 | 0.12000 | 0.12000 | $-5.2413\times10^{-09}$ |
| 50 | 1.00 | 44.9569 | 0.12000 | 0.12000 | $-9.6194\times10^{-11}$ |

The accuracy and effectiveness of the ADM are confirmed by using the error analysis given in Tables 1 and 2 followed by its MAE Figure 9(a,b) respectively. The other two Tables 3 and 4 confirm the errors that occur between the exact and approximate solution of the model. Their plots Figure 10(a,b) are shown, which are the graphical conformations for the error analysis between the two solutions (exact and approximate).

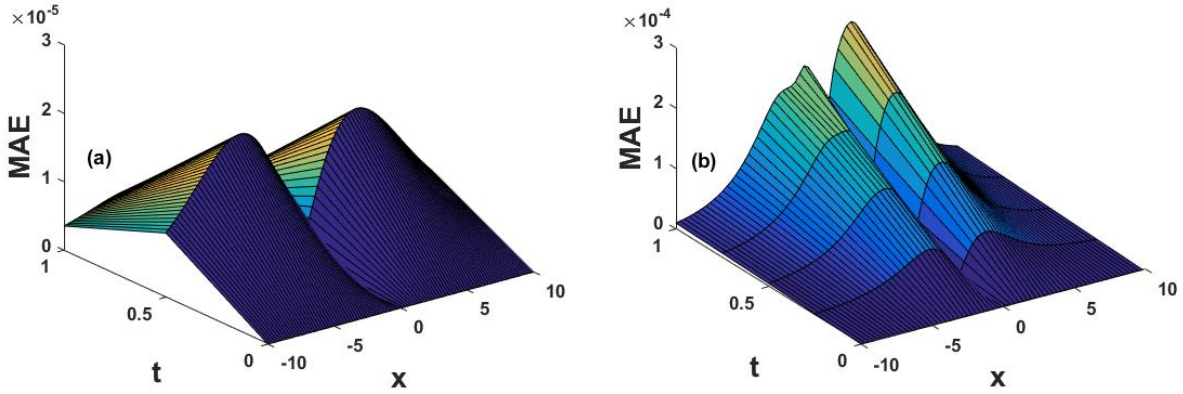


**Figure 9.** (a,b) 3D plots represent the mean absolute error (MAE) for different values of x and t for Tables 1 and 2 respectively.

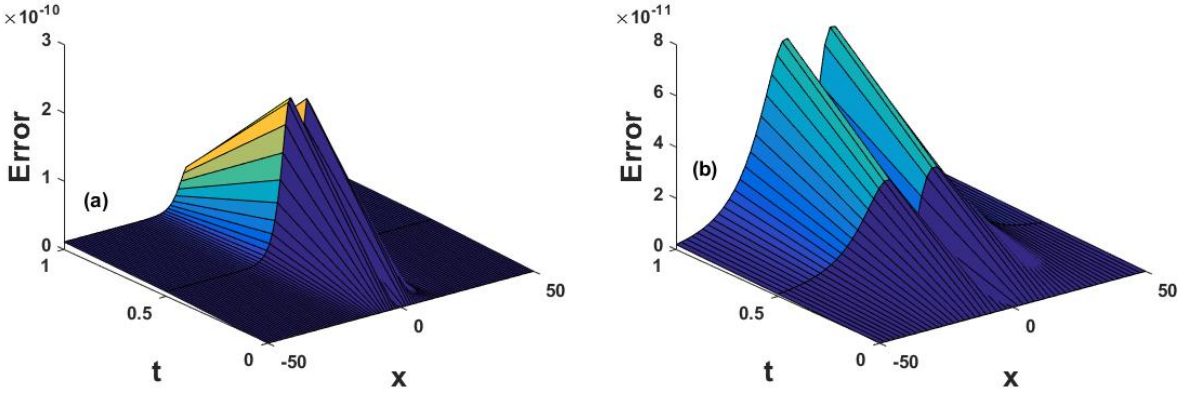


**Figure 10.** (a,b) 3D plots represent the mean absolute error (MAE) for different values of x and t for Tables 3 and 4 respectively.

## 6. Conclusions

We consider time-fractional Korteweg-de Vries (TF-KdV) and time-fractional modified Korteweg-de Vries (TF-mKdV) equations for solitary wave solutions with the help of an analytical method called the "Aboodh decomposition method (ADM)." The proposed method is a combination of the Aboodh transform and the decomposition method, which is a very authentic and valuable method for solving fractional-order non-linear problems. The approximate solution obtained with the help of ADM is compared with the exact solution of the models to verify the efficiency of the method. We observed from the graphical analysis in the manuscript the time-fractional order $\alpha$ can modify the wave profiles in such a way that when $\alpha$ values is increasing the amplitudes of the wave is reducing which is very much important to study the small amplitude's characteristics of such wave equations. The effect of the nonlinearity coefficient "a" and the dispersive coefficient "b" in Exp.1 are also discussed, form the graphical analysis we have shown that both of these coefficients have significant

affect on the wave amplitudes as well as its widths. We have studied the higher-order series solutions (up to fourth order) for time-fractional KdV and modified KdV equations with the help of the ADM. The convergence analysis determined that the obtained results are similar to the exact solutions of the models. The uniqueness results confirmed that ADM is an effective and systematic scheme for solving non-linear dynamical problems. The analytical and numerical solutions are plotted by marginal changes in parameters $x$, $t$ and $\alpha$. It is observed that a significant variation in the index values causes a large variation in the amplitude of the wave profile. For small-time $t$, the series solutions coincide with the exact solutions of the models, and the solutions are stable. However, for large-time $t$ the results show that the amplitudes of the wave profiles no longer remain constant at the given parameters. The results are tabulated for altered $x$, $t$ and $\alpha$. It is observed that mean absolute error (MAE) is decreasing for small-time and large values of $\alpha$ (fractional order). This means that for taking $\alpha$ values nearest to 1 (exact), the MAE values decrease, which means that the obtained results coincide with the solution of the considered models.

## 7. Future work

We studied the analytical solution of the TF-KdV and TF-mKdV equations with the help of ADM. The effectiveness of the proposed method is studied with the help of graphical analysis and some numerical error tables. The method is also essential for $K(m,n)$ equation obtained in [40]. Here, the author shows that $K(m,n)$ equations are only Lax integrable for specific values of the parameters $(\alpha, m, n)$. For the integrable instances, nontrivial prolongation structures and Lax pairings are provided.

## Acknowledgments

Princess Nourah bint Abdulrahman University Researchers Supporting Project number (PNURSP2022R8). Princess Nourah bint Abdulrahman University, Riyadh, Saudi Arabia.

## Conflict of interest

The authors declare that they have no conflicts of interest.

## References

1. D. Baleanu, K. Diethelm, E. Scalas, J. J. Trujillo, *Fractional calculus models and numerical methods*, World Scientific, 2012.
2. K. B. Oldham, J. Spanier, *Fractional calculus: Theory and applications of differentiation and integration to arbitrary order*, New York: Academic Press, 1974.
3. K. S. Miller, B. Ross, *An introduction to the fractional calculus and fractional differential equations*, New York, USA: John Wiley and Sons, 1993.
4. I. Podlubny, *Fractional differential equations*, San Diego, CA, USA: Academic Press, 1999.

5. J. A. T. Machado, A probabilistic interpretation of the fractional-order differentiation, *Fract. Calc. Appl. Anal.*, **6** (2003), 73–80.
6. R. L. Magin, M. Ovadia, Modeling the cardiac tissue electrode interface using fractional calculus, *J. Vib. Control*, **14** (2008), 1431–1442. https://doi.org/10.1177/10775463070874
7. K. S. Miller, B. Ross, *An introduction to the fractional calculus and fractional differential equations*, New York: Wiley, 1993.
8. D. J. Korteweg, On the change of form of long waves advancing in a rectangular canal and on a new type of long stationary waves, *Philos. Mag.*, **39** (1895), 73–80.
9. M. K. Fung, KdV Equation as an Euler-Poincare' equation, *Chin. J. Phys.*, **35** (1997), 789.
10. B. D. Fried, R. W. Gould, Longitudinal ion oscillations in a hot plasma, *Phys. Fluids*, **4** (1961), 139–147. https://doi.org/10.3390/math8020280
11. K. Watanabe, T. Taniuti, Electron-acoustic mode in a plasma of two-temperature electrons, *J. Phys. Soc. Japan*, **43** (1977), 1819–1820. https://doi.org/10.1143/JPSJ.43.1819
12. M. Y. Yu, P. K. Shukla, Linear and nonlinear modified electron-acoustic waves, *J. Plasma Phys.*, **29** (1983), 409–413. https://doi.org/10.1017/S0022377800000866
13. N. Iwamoto, Collective modes in nonrelativistic electron-positron plasmas, *Phys. Rev.*, **47** (1993), 604. https://doi.org/10.1103/PhysRevE.47.604
14. D. Henry, J. P. Trguier, Propagation of electronic longitudinal modes in a non-Maxwellian plasma, *J. Plasma Phys.*, **8** (1972), 311–319. https://doi.org/10.1017/S0022377800007169
15. R. Pottelette, R. E. Ergun, R. A. Treumann, M. Berthomier, C. W. Carlson, J. P. McFadden, et al., Modulated electron-acoustic waves in auroral density cavities: FAST observations, *Geophys. Res. Lett.*, **26** (1999), 2629–2632. https://doi.org/10.1029/1999GL900462
16. M. Irfan, I. Alam, A. Ali, K. Shah, T. Abdeljawad, Electron-acoustic solitons in dense electron-positron-ion plasma: Degenerate relativistic enthalpy function, *Results Phys.*, **38** (2022), 105625. https://doi.org/10.1016/j.rinp.2022.105625
17. H. Washimi, T. Taniuti, Propagation of ion-acoustic solitary waves of small amplitude, *Phys. Rev. Lett.*, **17** (1966), 996. https://doi.org/10.1103/PhysRevLett.17.996
18. E. K. El-Shewy, Effect of higher-order nonlinearity to nonlinear electron-acoustic solitary waves in an unmagnetized collisionless plasma, *Chaos Soliton. Fract.*, **26** (2005), 1073–1079. https://doi.org/10.1016/j.chaos.2005.01.060
19. E. K. El-Shewy, Linear and nonlinear properties of electron-acoustic solitary waves with non-thermal electrons, *Chaos Soliton. Fract.*, **31** (2007), 1020–1023. https://doi.org/10.1016/j.chaos.2006.03.104
20. R. M. Miura, C. S. Gardner, M. D. Kruskal, KdV equation and generalizations. II. Existence of conservation laws and constant of motion, *J. Math. Phys.*, **9** (1968), 1204–1209.
21. D. S. Wang, B. L. Guo, X. l. Wang, Long-time asymptotics of the focusing Kundu-Eckhaus equation with nonzero boundary conditions, *J. Differ. Equations*, **266** (2019), 5209–5253. https://doi.org/10.1016/j.jde.2018.10.053

22. D. S. Wang, L. Xu, Z. X. Xuan, The complete classification of solutions to the Riemann problem of the defocusing complex modified KdV equation, *J. Nonlinear Sci.*, **32** (2022), 1–46. https://doi.org/10.1007/s00332-021-09766-6

23. R. I. Nuruddeen, A. M. Nass, Aboodh decomposition method and its application in solving linear and vonlinear heat equations, *Eur. J. Adv. Eng. Technol.*, **3** (2016), 34–37.

24. K. S. Aboodh, The new integral transform'Aboodh transform, *Global J. Pure Appl. Math.*, **9** (2013), 35–43.

25. W. Cao, Y. Xu, Z. Zheng, Finite difference/collocation method for a generalized time-fractional KDV equation, *Appl. Sci.*, **8** (2018), 42. https://doi.org/10.3390/app8010042

26. D. Kaya, I. E. Inan, A convergence analysis of the ADM and an application, *Appl. Math. Comput.*, **161** (2005), 1015–1025. https://doi.org/10.1016/j.amc.2003.12.063

27. S. A. El-Wakil, E. M. Abulwafa, E. K. El-Shewy, A. A. Mahmoud, Time-fractional KdV equation for plasma of two different temperature electrons and stationary ion, *Phys. Plasmas*, **18** (2011), 092116. https://doi.org/10.1063/1.3640533

28. A. Atangana, D. Baleanu, New fractional derivatives with nonlocal and non-singular kernel: Theory and application to heat transfer model, *Therm Sci.*, *Phys. Plasmas*, **20** (2016), 763–769. https://doi.org/10.48550/arXiv.1602.03408

29. K. Khan, O. Algahtani, M. Irfan, A. Ali, Electron-acoustic solitary potential in nonextensive streaming plasm, *Sci. Rep.*, **12** (2022), 15175. https://doi.org/10.1038/s41598-022-19206-4

30. K. Khan, Z. Khan, A. Ali, M. Irfan, Investigation of Hirota equation: Modified double Laplace decomposition method, *Phys. Scr.*, **96** (2021), 104006. https://doi.org/10.1088/1402-4896/ac0d33

31. A. Atangana, Extension of the modified homotopy perturbation method for attractor one-dimensional Keller-Segel equations, *Appl. Math. Model.*, **39** (2015), 2815–3182. https://doi.org/10.1016/j.apm.2014.09.029

32. K. S. Aboodh, The new integral transform "Aboodh transform", *Global J. Pure Appl. Math.*, **9** (2013), 35–43.

33. S. Alfaqeih, T. Ozis, Note on double Aboodh transform of fractional order and its properties, *Online Math. OMJ*, **1** (2019), 19–25. https://doi.org/10.5281/zenodo.3047015

34. A. A. Kilbas, H. M. Srivastava, J. J. Trujillo, *Theory and applications of fractional differential equations*, Elsevier, 2006.

35. R. Aruldoss, R. A. Devi, Aboodh transform for solving fractional differential equations, *Global J. Pure Appl. Math.*, **16** (2020), 145–153.

36. G. Adomian, Modification of the decomposition approach to heat equation, *J. Math. Anal. Appl.*, **124** (1987), 290–291. https://doi.org/10.1016/0022-247X(87)90040-0

37. I. L. El-Kalla, Convergence of the Adomian method applied to a class of nonlinear integral equations, *Appl. Math. Lett.*, **21** (2008), 372–376. https://doi.org/10.1016/j.aml.2007.05.008

38. H. Eltayeb, Y. T. Abdalla, I. Bachar, M. H. Khabir, Fractional telegraph equation and its solution by natural transform decomposition method, *Symmetry*, **11** (2019), 334. https://doi.org/10.3390/sym11030334

39. Q. Wang, Homotopy perturbation method for fractional KdV equation, *Appl. Math. Comput.*, **190** (2007), 1795–1802. https://doi.org/10.1016/j.amc.2007.02.065

40. D. S. Wang, S. Y. Lou, Prolongation structures and exact solutions of $K(m, n)$ equations, *J. Math. Phys.*, **50** (2009), 123513. https://doi.org/10.1063/1.3267865


AIMS Press